THE ASTROPHYSICAL JOURNAL, 536:1–18, 2000 June 10

GAMMA-RAY BURSTS AS A PROBE OF THE VERY HIGH REDSHIFT UNIVERSE

DONALD Q. LAMB AND DANIEL E. REICHART
Department of Astronomy and Astrophysics, University of Chicago, 5640 South Ellis Avenue, Chicago, IL 60637; lamb@oddjob.uchicago.edu
Received 1999 September 10; accepted 2000 January 20

ABSTRACT

There is increasingly strong evidence that gamma-ray bursts (GRBs) are associated with star-forming galaxies and occur near or in the star-forming regions of these galaxies. These associations provide indirect evidence that at least the long GRBs detected by *BeppoSAX* are a result of the collapse of massive stars. The recent evidence that the light curves and the spectra of the afterglows of GRB 970228 and GRB 980326 appear to contain a supernova component, in addition to a relativistic shock-wave component, provides more direct clues that this is the case. We show that, if many GRBs are indeed produced by the collapse of massive stars, GRBs and their afterglows provide a powerful probe of the very high redshift ($z \gtrsim 5$) universe. We first establish that GRBs and their afterglows are both detectable out to very high redshifts. We then show that one expects GRBs to occur out to at least $z \approx 10$, and possibly to $z \approx 15$–20, redshifts that are far larger than those expected for the most distant quasars. This implies that there are large numbers of GRBs with peak photon number fluxes below the detection thresholds of BATSE and *HETE* 2, and even below the detection threshold of *Swift*. The mere detection of very high redshift GRBs would give us our first information about the earliest generations of stars. We show that GRBs and their afterglows can be used as beacons to locate core-collapse supernovae at redshifts $z \gg 1$ and to study the properties of these supernovae. We describe the expected properties of the absorption-line systems and the Lyα forest in the spectra of GRB afterglows and discuss various strategies for determining the redshifts of very high redshift GRBs. We then show how the absorption-line systems and the Lyα forest visible in the spectra of GRB afterglows can be used to trace the evolution of metallicity in the universe and to probe the large-scale structure of the universe at very high redshifts. Finally, we show how measurement of the Lyα break in the spectra of GRB afterglows can be used to constrain, or possibly measure, the epoch at which reionization of the universe occurred by using the Gunn-Peterson test.

Subject headings: cosmology: theory — galaxies: abundances — gamma rays: bursts — large-scale structure of universe — stars: formation — supernovae: general

1. INTRODUCTION

The relatively accurate (3′) gamma-ray burst (GRB) positions found using *BeppoSAX* and disseminated within a day or so led to the remarkable discoveries that GRBs have X-ray (Costa et al. 1997), optical (Galama et al. 1997), and radio (Frail & Kulkarni 1997) afterglows. The redshift distances of eight GRBs are currently known, either directly from absorption lines in the spectra of the afterglow or indirectly from emission lines in the spectra of a galaxy that is coincident with the position of the X-ray and optical afterglow. These redshifts span the range $z = 0.43$–3.42 and imply that GRBs are perhaps the most luminous and energetic events in the universe (see Table 1).

The most widely discussed models of the central engine of GRBs involve a black hole and an accretion disk, formed either through the core collapse of a massive star (Woosley 1993, 1996; Paczyński 1998; MacFadyen & Woosley 1999; Wheeler et al. 2000; MacFadyen, Woosley, & Heger 1999) or the coalescence of a neutron star/neutron star or neutron star/black hole binary (Paczyński 1986; Narayan, Paczyński, & Piran 1992; Mészáros & Rees 1992). The former are expected to occur near or in the star-forming regions of their host galaxies, while most of the latter are expected to occur primarily outside of the galaxies in which they were born.

Castander & Lamb (1998) showed that the light from the host galaxy of GRB 970228, the first burst for which an afterglow was detected, is very blue. This implies that the host galaxy is undergoing copious star formation and suggests an association between GRB sources and star-forming galaxies. Subsequent analyses of the color of this galaxy (Castander & Lamb 1999; Fruchter et al. 1999a) and other host galaxies (Kulkarni et al. 1998; Fruchter 1999) have strengthened this conclusion, as has the detection of [O II] and Lyα emission lines from several host galaxies (see, e.g., Metzger et al. 1997a; Kulkarni et al. 1998; Bloom et al. 1998).

The positional coincidences between burst afterglows and the bright blue regions of the host galaxies (Sahu et al. 1997; Kulkarni et al. 1998; Fruchter 1999; Kulkarni et al. 1999; Fruchter et al. 1999a), and the evidence for extinction by dust of some burst afterglows (see, e.g., Reichart 1998; Kulkarni et al. 1998; Lamb, Castander, & Reichart 1999), lend further support to the idea that GRBs are associated with star formation, as is expected if GRBs are caused by the collapse of massive stars. However, this evidence is indirect.

Recent tantalizing evidence that the light curves and spectra of the afterglows of GRB 980326 (Bloom et al. 1999) and GRB 970228 (Reichart 1999; Galama et al. 1999b) contain a supernova (SN) component, in addition to a relativistic shock-wave component, provide more direct clues that at least the long, softer, smoother bursts (Lamb, Graziani, & Smith 1993; Kouveliotou et al. 1993) detected by *BeppoSAX* are a result of the collapse of massive stars.

TABLE 1

PEAK PHOTON FLUXES AND ISOTROPIC LUMINOSITIES FOR GRBs WITH SECURE REDSHIFTS

GRB	Redshift	P (photons cm^{-2} s^{-1})[a]	L_P (photons s^{-1})[b]	Redshift Reference
970228	0.695	3.5	5.1×10^{57}	1
970508	0.835	1.2	2.5×10^{57}	2, 3
971214	3.418	2.3	6.4×10^{58}	4
980613	1.096	0.63	2.3×10^{57}	5
980703	0.967	2.6	7.4×10^{57}	6
990123	1.600	16.4	1.2×10^{59}	7
990510	1.619	8.16	6.2×10^{58}	8
990712[c]	0.430	...	...	9

[a] From J. Norris (http://cossc.gsfc.nasa.gov/cossc/batse/counterparts). The listed peak photon flux is that in the energy band 50–300 keV.

[b] Assuming $H_0 = 65$ km s^{-1} Mpc^{-1}, $\Omega_m = 0.3$, and $\Omega_\Lambda = 0.7$.

[c] Peak photon flux not yet reported.

REFERENCES. — (1) Djorgovski et al. 1999b; (2) Metzger et al. 1997a; (3) Metzger et al. 1997b; (4) Kulkarni et al. 1998; (5) Djorgovski et al. 1999a; (6) Djorgovski et al. 1998; (7) Kulkarni et al. 1999; (8) Vreeswijk et al. 1999; (9) Galama et al. 1999a.

This paper shows that, if many GRBs are indeed produced by the collapse of massive stars, GRBs and their afterglows provide a powerful probe of the very high redshift ($z \gtrsim 5$) universe. In § 2, we establish that both GRBs and their afterglows are detectable out to very high redshifts. In § 3, we then show that one expects GRBs to occur out to $z \approx 10$ and possibly $z \approx 15$–20, redshifts that are far larger than those expected for the most distant quasars. This implies that there are large numbers of GRBs with peak photon number fluxes below the detection thresholds of BATSE and *HETE* 2, and even below the detection threshold of *Swift*. The mere detection of very high redshift GRBs would give us our first information about the earliest generations of stars. In § 4, we show that GRBs and their afterglows can be used as beacons to locate core-collapse supernovae at redshifts $z \gg 1$ and to study the properties of these supernovae. In § 5, we describe the expected properties of the absorption-line systems and the Lyα forest in the spectra of GRB afterglows and discuss various strategies for determining the redshifts of very high redshift GRBs. We then show in § 6 how the absorption-line systems and the Lyα forest visible in the spectra of GRB afterglows can be used to trace the evolution of metallicity in the universe and, in § 7, how they can be used to probe the large-scale structure of the universe at very high redshifts. Finally, in § 8, we show how measurement of the Lyα break in the spectra of GRB afterglows can be used to constrain, or possibly measure, the epoch at which reionization of the universe occurred using the Gunn-Peterson test. We summarize our conclusions in § 9.

2. DETECTABILITY OF GRBs AND THEIR AFTERGLOWS AT VERY HIGH REDSHIFTS

It is now clear that GRBs are detectable out to very high redshifts (VHRs). To establish this, we calculate the limiting redshifts detectable by BATSE and *HETE* 2, and by *Swift*, for the seven GRBs with well-established redshifts and published peak photon number fluxes. The peak photon number luminosity is

$$L_P = \int_{\nu_l}^{\nu_u} \frac{dL_P}{d\nu}\, d\nu\ , \tag{1}$$

where $\nu_l < \nu < \nu_u$ is the band of observation. Typically, for the Burst and Transient Source Experiment (BATSE) on the *Compton Gamma-Ray Observatory*, (*CGRO*) $\nu_l = 50$ keV and $\nu_u = 300$ keV. The corresponding peak photon number flux P is

$$P = \int_{\nu_l}^{\nu_u} \frac{dP}{d\nu}\, d\nu\ . \tag{2}$$

Assuming that GRBs have a photon number spectrum of the form $dL_P/d\nu \propto \nu^{-\alpha}$ and that L_P is independent of z, the observed peak photon number flux P for a burst occurring at a redshift z is given by

$$P = \frac{L_P}{4\pi D^2(z)(1+z)^\alpha}\ , \tag{3}$$

where

$$D(z) = c\int_0^z (1+z')\left|\frac{dt(z')}{dz'}\right| dz' \tag{4}$$

is the comoving distance to the GRB, and

$$\frac{dt(z)}{dz} = -\left(\frac{c}{H_0}\right)\{(1+z)[\Omega_m(1+z)^3 + \Omega_\Lambda + (1-\Omega_m-\Omega_\Lambda)(1+z)^2]^{1/2}\}^{-1}\ . \tag{5}$$

Throughout this paper, we take $\Omega_m + \Omega_\Lambda = 1$. Then

$$D(z) = \frac{c}{H_0} \int_0^z \frac{dz'}{\sqrt{\Omega_m (1 + z')^3 + \Omega_\Lambda}} . \tag{6}$$

Taking $\alpha = 1$, which is typical of GRBs (Mallozzi, Pendleton, & Paciesas 1996),

$$P = \frac{L_P}{4\pi D^2(z)(1 + z)} , \tag{7}$$

which is coincidentally identical to the form one gets when P and L_P are bolometric quantities.

Using these expressions, we have calculated the limiting redshifts detectable by BATSE and *HETE 2*, and by *Swift*, for the seven GRBs with well-established redshifts and published peak photon number fluxes. In doing so, we have used the peak photon number fluxes given in Table 1, taken a detection threshold of 0.2 photons s^{-1} for BATSE (Paciesas et al. 1999) and *HETE 2* (Ricker 1998) and 0.04 photons s^{-1} for *Swift* (Gehrels 1999), and set $H_0 = 65$ km s^{-1} Mpc^{-1}, $\Omega_m = 0.3$, and $\Omega_\Lambda = 0.7$ (other cosmologies give similar results).

Figure 1 displays the results. This figure shows that BATSE and *HETE 2* would be able to detect four of these GRBs (GRBs 970228, 970508, 980613, and 980703) out to redshifts $2 \lesssim z \lesssim 4$, and three (GRBs 971214, 990123, and 990510) out to redshifts of $20 \lesssim z \lesssim 30$. *Swift* would be able to detect the former four out to redshifts of $5 \lesssim z \lesssim 15$ and the latter three out to redshifts in excess of $z \approx 70$, although it is unlikely that GRBs occur at such extreme redshifts (see § 3 below). Consequently, if GRBs occur at VHRs, BATSE has probably detected them already, and future missions should detect them as well.

The soft X-ray, optical, and infrared afterglows of GRBs are also detectable out to VHRs. The effects of distance and redshift tend to reduce the spectral flux in GRB afterglows in a given frequency band, but time dilation tends to increase it at a fixed time of observation after the GRB since afterglow intensities tend to decrease with time. These effects combine to produce little or no decrease in the spectral energy flux F_ν of GRB afterglows in a given frequency band and at a fixed time of observation after the GRB with increasing redshift:

$$F_\nu(\nu, t) = \frac{L_\nu(\nu, t)}{4\pi D^2(z)(1 + z)^{1 - a + b}} , \tag{8}$$

where $L_\nu \propto \nu^a t^b$ is the intrinsic spectral luminosity of the GRB afterglow, which we assume applies even at early times, and $D(z)$ is again the comoving distance to the burst. Many afterglows fade like $b \approx -4/3$, which implies that $F_\nu(\nu, t) \propto D(z)^{-2} (1 + z)^{-5/9}$ in the simplest afterglow model where $a = 2b/3$ (see, e.g., Wijers, Rees, & Mészáros 1997). In addition, $D(z)$ increases very slowly with redshift at redshifts greater than a few. Consequently, there is little or no decrease in the spectral flux of GRB afterglows with increasing redshift beyond $z \approx 3$.

For example, Halpern et al. (1999) find in the case of GRB 980519 that $a = -1.05 \pm 0.10$ and $b = -2.05 \pm 0.04$, so that $1 - a + b = 0.00 \pm 0.11$, which implies no decrease in the spectral flux with increasing redshift, except for the effect of $D(z)$. In the simplest afterglow model where $a = 2b/3$, if the afterglow declines more rapidly than $b \approx 1.7$, the spectral flux actually *increases* as one moves the burst to higher redshifts!

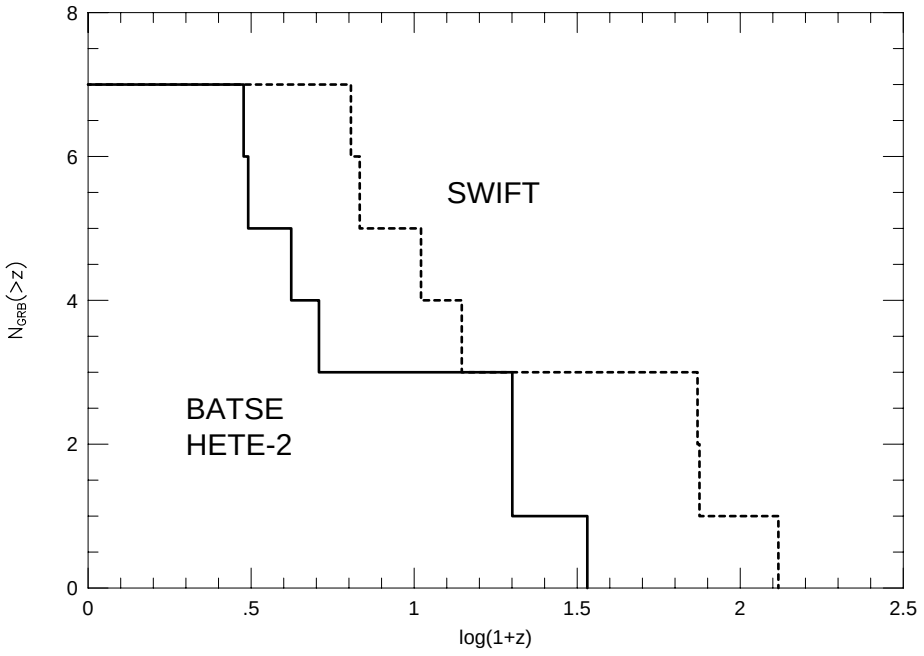

FIG. 1.—Cumulative distributions of the limiting redshifts at which the seven GRBs with well-determined redshifts and published peak photon number fluxes would be detectable by BATSE and *HETE 2*, and by *Swift*.

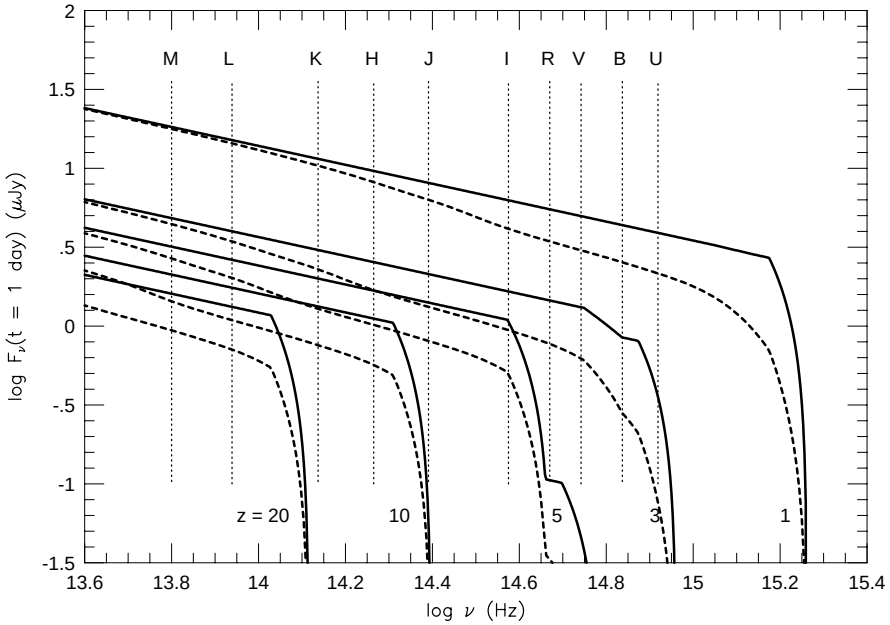

FIG. 2.—Best-fit light curve of the early afterglow of GRB 970228 from Reichart (1999) transformed to various redshifts

As another example, we calculate the best-fit spectral flux distribution of the early afterglow of GRB 970228 from Reichart (1999), as observed one day after the burst, transformed to various redshifts. The transformation involves (1) dimming the afterglow,[1] (2) redshifting its spectrum, (3) time dilating its light curve, and (4) extincting the spectrum using a model of the Lyα forest. For the model of the Lyα forest, we have adopted the best-fit flux deficit distribution to Sample 4 of Zuo & Lu (1993) from Reichart (2000). At redshifts in excess of $z = 4.4$, this model is an extrapolation, but it is consistent with the results of theoretical calculations of the redshift evolution of Lyα absorbers (see, e.g., Valageas, Schaeffer, & Silk 1999). Finally, we have convolved the transformed spectra with a top-hat smearing function of width $\Delta\nu = 0.2\nu$. This models these spectra as they would be sampled photometrically, as opposed to spectroscopically; i.e., this transforms the model spectra into model spectral flux distributions.

Figure 2 shows the resulting K-band light curves. For a fixed band and time of observation, steps (1) and (2) above dim the afterglow and step (3) brightens it, as discussed above. Figure 2 shows that in the case of the early afterglow of GRB 970228, as in the case of GRB 980519, at redshifts greater than a few, the three effects nearly cancel one another out. Thus the afterglow of a GRB occurring at a redshift slightly in excess of $z = 10$ would be detectable at $K \approx 16.2$ mag one hour after the burst and at $K \approx 21.6$ mag one day after the burst, if its afterglow were similar to that of GRB 970228 (a relatively faint afterglow).

Figure 3 shows the resulting spectral flux distribution. The spectral flux distribution of the afterglow is cut off by the Lyα forest at progressively lower frequencies as one moves out in redshift. Thus high redshift ($1 \lesssim z \lesssim 5$) afterglows are characterized by an optical "dropout" (Fruchter 1999) and very high redshift ($z \gtrsim 5$) afterglows by an infrared "dropout."

We also show in Figure 3 the effect of a moderate ($A_V = \frac{1}{3}$), fixed amount of extinction at the redshift of the GRB. However, the amount of extinction is likely to be very small at large redshifts because of the rapid decrease in metallicity beyond $z = 3$ (see § 6 below).

So far, optical observations have been favored over near-infrared (NIR) and IR observations in afterglow searches. This is understandable, given the greater availability of optical cameras and the modest (typically $2' \times 2'$) fields of view of current NIR cameras. Usually, deep NIR observations have been carried out only once an optical transient has been identified in a GRB error circle, thereby assuring that the afterglow can be captured within the field of view of the NIR camera. The K-band afterglow search of Gorosabel et al. (1998), which detected the afterglow of GRB 971214 only 3.2 hr after the burst, is a notable exception. Unfortunately, the current search strategy of waiting for the identification of an afterglow candidate at optical wavelengths before carrying out NIR observations biases against the identification of VHR GRBs since the afterglows of these bursts cannot be detected at optical wavelengths.

The results of our calculations show that the identification of VHR GRBs will require afterglow searches that incorporate on a consistent basis (1) sufficiently deep NIR observations, carried out within hours to days after the burst, and (2) near-simultaneous optical observations that go sufficiently deep to meaningfully constrain the redshift of the burst in the event that its afterglow is detected only at NIR wavelengths. Fortunately, early NIR observations will be facilitated by the *HETE 2* (Ricker 1998) and *Swift* missions (Gehrels 1999), which will provide positions accurate to better than several arcminutes for many GRBs in near-real time.

For more than half of the nearly two dozen GRBs for which X-ray afterglows have been detected, a corresponding optical afterglow has not been detected. A possible explanation of this "missing optical afterglow" problem is that, because of larger positional error circles or other reasons, optical afterglow searches do not always go deep enough, soon enough, to detect the

[1] Again, we have set $\Omega_m = 0.3$ and $\Omega_\Lambda = 0.7$; other cosmologies yield similar results.

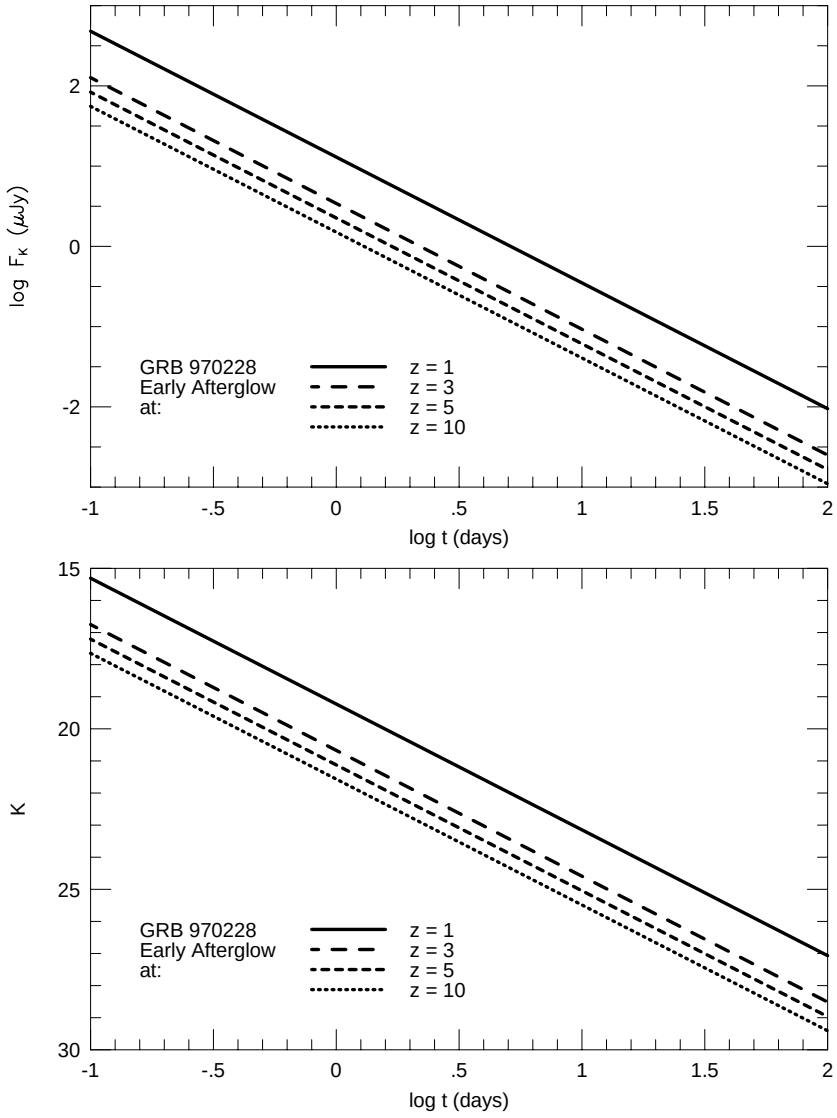

FIG. 3.—Best-fit spectral flux distribution of the early afterglow of GRB 970228 from Reichart (1999), as observed one day after the burst, after transforming it to various redshifts and extincting it with a model of the Lyα forest. Dashed curves are extincted versions of the solid curves, where we have adopted $A_V = \frac{1}{3}$ mag at the redshift of the burst and an extinction curve typical of the interstellar medium of our Galaxy.

fading afterglows. This may explain many of the missing optical afterglows, but it probably does not account for all of them. Another possible explanation is that some of these afterglows are significantly extincted by dust, either in our Galaxy, in the host galaxies, or in the environments immediate to the bursts themselves (see, e.g., Reichart 1998, 2000). Finally, it is possible that some of the GRBs for which no optical afterglow has been detected occurred at VHRs, and therefore their afterglow spectra were absorbed in the optical, as described above. In reality, a combination of these three effects may be at work. Early *HST* and NIR afterglow searches, facilitated by the more accurate near-real time positions that the *HETE 2* and *Swift* missions will provide, could help to distinguish between these various explanations.

In conclusion, if GRBs occur at very high redshifts, both they and their afterglows would be detectable.

3. GRB AFTERGLOWS AS A PROBE OF STAR FORMATION

The positional coincidences between burst afterglows and the bright blue regions of the host galaxies (Sahu et al. 1997; Kulkarni et al. 1998; Fruchter 1999; Kulkarni et al. 1999; Fruchter et al. 1999a), and the evidence for extinction by dust of some burst afterglows (see, e.g., Reichart 1998; Kulkarni et al. 1998; Lamb et al. 1999), lends support to the idea that GRBs are associated with star formation.

The discovery of what appears to be supernova components in the afterglows of GRB 970228 (Reichart 1999; Galama et al. 1999b) and GRB 980326 (Bloom et al. 1999) strongly suggests that at least some GRBs are related to the deaths of massive stars, as predicted by the widely discussed collapsar model of GRBs (see, e.g., Woosley 1993, 1996; Paczyński 1998; MacFadyen & Woosley 1999; Wheeler et al. 2000; MacFadyen et al. 1999). The presence of an unusual radio supernova, SN 1998bw, in the error circle of GRB 980425 (Galama et al. 1998; Kulkarni et al. 1998) also lends support to this hypothesis, although the identification of SN 1998bw with GRB 980425 is not secure (see, e.g., Graziani, Lamb, & Marion 1999). If GRBs are related to the collapse of massive stars, one expects the GRB rate to be approximately proportional to the star formation rate (SFR).

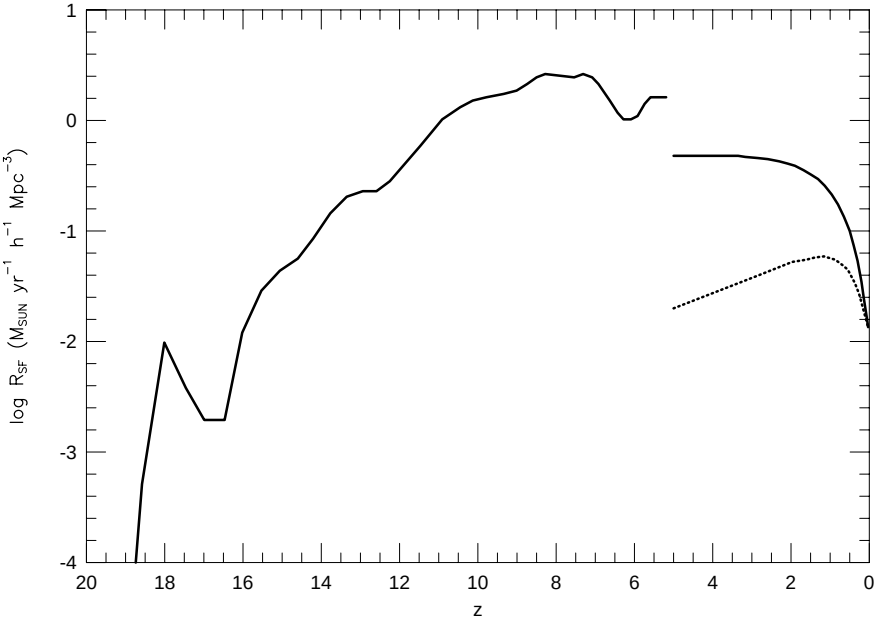

FIG. 4.—Cosmic star formation rate R_{SF} as a function of redshift z. The solid curve at $z < 5$ is the SFR derived by Rowan-Robinson (1999) from submillimeter, infrared, and UV data; the solid curve at $z \geq 5$ is the SFR calculated by Gnedin & Ostriker (1997). The dip in this curve at $z \approx 6$ is an artifact of their numerical simulation (Gnedin & Ostriker 1997). The dotted curve is the SFR derived by Madau et al. (1998).

Observational estimates (Gallego et al. 1995; Lilly et al. 1996; Connolly et al. 1997; Madau, Pozzetti, & Dickinson 1998) indicate that the SFR in the universe was about 15 times larger at a redshift $z \approx 1$ than it is today. The data at higher redshifts from the Hubble Deep Field (HDF) in the north suggests a peak in the SFR at $z \approx 1$–2 (Madau et al. 1998), but the actual situation is highly uncertain. Assuming that GRBs are standard candles and the estimate of the SFR derived by Madau et al. (1998; however, see Pei, Fall, & Hauser 1999), several authors (Totani 1997, 1999; Wijers et al. 1998) have investigated whether or not the observed GRB brightness distribution is consistent with such a SFR, which rises rapidly from the present epoch and peaks at $z \approx 1$–2. Totani (1997, 1999) finds that it is not, and one can infer from the results of Wijers et al. (1998) that it is not.

However, there is now overwhelming evidence that GRBs are not standard candles. The peak photon number fluxes P of the seven GRBs with secure redshifts and published peak photon fluxes span nearly 2 orders of magnitude (see Table 1). The range of peak photon number fluxes may actually be much greater (Loredo & Wasserman 1998). Furthermore, theoretical calculations show that the birthrate of Population III stars produces a peak in the SFR in the universe at redshifts $16 \lesssim z \lesssim 20$ while the birthrate of Population II stars produces a much larger and broader peak at redshifts $2 \lesssim z \lesssim 10$ (Ostriker & Gnedin 1996; Gnedin & Ostriker 1997; Valageas & Silk 1999). Consequently, if GRBs are produced by the collapse of massive stars in binaries, one expects them to occur out to at least $z \approx 10$ and possibly to $z \approx 15$–20, redshifts that are far larger than those expected for the most distant quasars.

Therefore, if GRBs—or at least a well-defined subset of the observed GRBs, such as the long bursts—are caused by the deaths of massive stars, as theory and observations now suggest, then GRBs are a powerful probe of the star formation history of the universe, and particularly of the SFR at VHRs. In Figure 4, we have plotted the SFR versus redshift from a phenomenological fit (Rowan-Robinson 1999) to the SFR derived from submillimeter, infrared, and UV data at redshifts $z < 5$ and from a numerical simulation by Gnedin & Ostriker (1997; see Fig. 2*b* of their paper) at redshifts $z \geq 5$. The simulations done by Gnedin & Ostriker (1997) indicate that the SFR increases with increasing redshift until $z \approx 10$, at which point it levels off. The smaller peak in the SFR at $z \approx 18$ corresponds to the formation of Population III stars, brought on by cooling by molecular hydrogen. In their other simulations, the strength of this peak was found to be greater than in the example used here (Ostriker & Gnedin 1996; Gnedin & Ostriker 1997). Since GRBs are detectable at these VHRs (see § 2) and their redshifts may be measurable from the absorption-line systems and the Lyα break in the afterglows (see § 5 below), if the GRB rate is proportional to the SFR, then GRBs could provide unique information about the star formation history of the VHR universe.

More easily but less informatively, one can examine the GRB peak photon flux distribution $N_{GRB}(P)$. To illustrate this, we have calculated the expected GRB peak flux distribution assuming (1) that the GRB rate is proportional to the star formation rate,[2] (2) that the star formation rate is that given in Figure 4, and (3) that the peak photon luminosity distribution $f(L_P)$ of the bursts is independent of z. There is a mismatch of about a factor of 3 between the $z < 5$ and $z \geq 5$ regimes. However, estimates of the star formation rate are uncertain by at least this amount in both regimes. We have chosen therefore to match the two regimes smoothly to one another to avoid creating a discontinuity in the GRB peak flux distribution that would be entirely an artifact of this mismatch.

[2] This may underestimate the GRB rate at VHRs since it is generally thought that the initial mass function will be tilted toward a greater fraction of massive stars at VHRs because of less efficient cooling caused by the lower metallicity of the universe at these early times.

We calculate the observed GRB peak photon flux distribution $N_{\rm GRB}(P)$ as follows. Assuming that GRBs are standard candles of peak photon luminosity L_P, the peak photon flux distribution is

$$N_{\rm GRB}(P \mid L_P) = \Delta T_{\rm obs} \frac{R_{\rm SF}(z)}{1+z} \frac{dV(z)}{dz} \left| \frac{dz(P \mid L_P)}{dP} \right| , \tag{9}$$

where $\Delta T_{\rm obs}$ is the length of time of observation, $R_{\rm SF}(z)$ is the local comoving star formation rate at z,

$$\frac{dV(z)}{dz} = 4\pi \frac{d_L^2(z)}{1+z} \left| \frac{dt(z)}{dz} \right| \tag{10}$$

is the differential comoving volume,

$$d_L(z) = \begin{cases} \dfrac{c}{H_0\sqrt{1-\Omega_m-\Omega_\Lambda}}(1+z)\sinh\left[\dfrac{H_0\sqrt{1-\Omega_m-\Omega_\Lambda}}{c}D(z)\right] & (\Omega_m+\Omega_\Lambda<1) \\ (1+z)D(z) & (\Omega_m+\Omega_\Lambda=1) \\ \dfrac{c}{H_0\sqrt{\Omega_m+\Omega_\Lambda-1}}(1+z)\sin\left[\dfrac{H_0\sqrt{\Omega_m+\Omega_\Lambda-1}}{c}D(z)\right] & (\Omega_m\,G489+\Omega_\Lambda>1) \end{cases} \tag{11}$$

is the luminosity distance, and

$$\frac{dz(P \mid L_P)}{dP} = \left[\frac{dP(z \mid L_P)}{dz}\right]^{-1} . \tag{12}$$

For $\Omega_m + \Omega_\Lambda = 1$,

$$\frac{dV(z)}{dz} = 4\pi D^2(z) \frac{dD(z)}{dz} , \tag{13}$$

where the comoving distance

$$D(z) = \frac{c}{H_0}\int_0^z \frac{dz'}{[\Omega_m(1+z')^3+\Omega_\Lambda]^{1/2}} , \tag{14}$$

and

$$\frac{dD(z)}{dz} = \frac{c}{H_0}\frac{1}{[\Omega_m(1+z)^3+\Omega_\Lambda]^{1/2}} . \tag{15}$$

For $dL_P/dv \propto v^{-\alpha}$,

$$P(z \mid L_P) = \frac{L_P}{4\pi D^2(z)(1+z)^\alpha} . \tag{16}$$

Again taking $\alpha = 1$, which is typical of GRBs (Mallozzi et al. 1996),

$$P(z \mid L_P) = \frac{L_P}{4\pi D^2(z)(1+z)} . \tag{17}$$

Then

$$\left| \frac{dP(z \mid L_P)}{dz} \right| = \frac{L_P}{4\pi}\left[\frac{2}{D^3(z)(1+z)}\frac{dD(z)}{dz} + \frac{1}{D^2(z)(1+z)^2}\right] . \tag{18}$$

For a luminosity function $f(L_P)$ and for $dL_P/dv \propto v^{-\alpha}$, $N_{\rm GRB}(P)$ is given by the following convolution integration:

$$N_{\rm GRB}(P) = \Delta T_{\rm obs}\int_0^\infty R_{\rm GRB}(P \mid L_P) f[L_P - 4\pi D^2(z)(1+z)^\alpha P] dL_P . \tag{19}$$

The upper panel of Figure 5 shows the number $N_*(z)$ of stars expected as a function of redshift z (i.e., the star formation rate, weighted by the comoving volume and time-dilated) for an assumed cosmology $\Omega_M = 0.3$ and $\Omega_\Lambda = 0.7$ (other cosmologies give similar results). The solid curve corresponds to the SFR in Figure 4. The dashed curve corresponds to the SFR derived by Madau et al. (1998). This figure shows that $N_*(z)$ peaks sharply at $z \approx 2$ and then drops off fairly rapidly at higher z, with a tail that extends out to $z \approx 12$. The rapid rise in $N_*(z)$ out to $z \approx 2$ is caused by the rapidly increasing volume of space. The rapid decline beyond $z \approx 2$ is almost completely because of the "edge" in the spatial distribution produced by the cosmology. In essence, the sharp peak in $N_*(z)$ at $z \approx 2$ reflects that the SFR we have taken is fairly broad in z and, consequently, the behavior of $N_*(z)$ is dominated by the behavior of the comoving volume $dV(z)/dz$; i.e., the shape of $N_*(z)$ is caused almost entirely by cosmology. The lower panel in Figure 5 shows the cumulative distribution $N_*(>z)$ of the number of stars

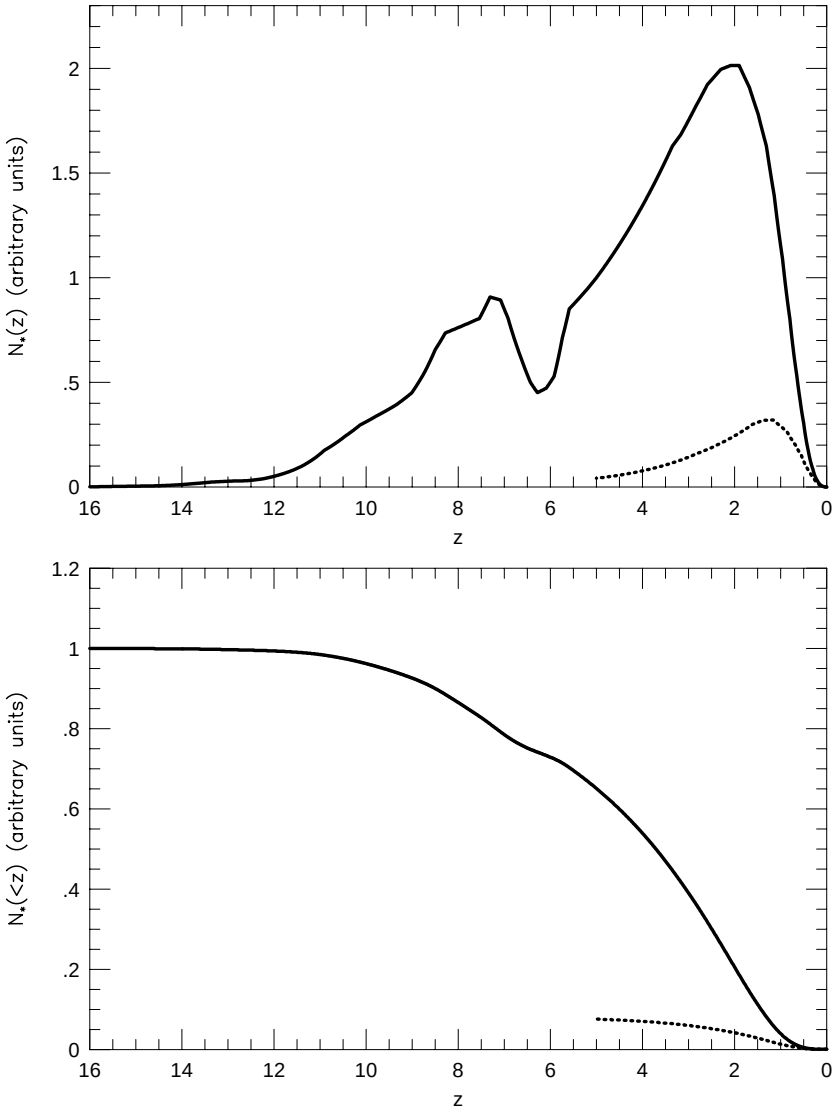

FIG. 5.—*Top panel:* Number N_* of stars expected as a function of redshift z (i.e., the SFR from Fig. 4, weighted by the differential comoving volume and time-dilated) assuming that $\Omega_M = 0.3$ and $\Omega_\Lambda = 0.7$. The solid and dashed curves, and the dip in the solid curve at $z \approx 6$, have the same meanings as in Fig. 4. *Bottom panel:* Cumulative distribution of the number N_* of stars expected as a function of redshift z. Again, the solid and dashed curves have the same meanings as in Fig. 4. Note that $\approx 40\%$ of all stars have redshifts $z > 5$.

expected as a function of redshift z. The solid and dashed curves have the same meaning as in the upper panel. This figure shows that $\approx 40\%$ of all stars have redshifts $z > 5$.

The upper panels of Figures 6, 7, and 8 show the predicted peak photon flux distribution $N_{\rm GRB}(P)$. The solid curve assumes that all bursts have a peak (isotropic) photon luminosity $L_P = 10^{58}$ photons s^{-1}. However, as remarked above, there is now overwhelming evidence that GRBs are not "standard candles." Consequently, we also show in Figures 6–8, as illustrative examples, the convolution of this same SFR and a photon luminosity function,

$$f(L_P) \propto \begin{cases} L_P^{-\beta} & L_{\rm min} < L_P < L_{\rm max} \\ 0 & \text{otherwise} \end{cases}, \tag{20}$$

where ($\log L_{\rm min}$, $\log L_{\rm max}$) = (57.5, 58.5), (57, 59), and (56.5, 59.5); i.e., $f(L_P)$ is centered on $L_P = 10^{58}$ photons s^{-1} and has widths $\Delta L_P/L_P = 10$, 100, and 1000.[3] The actual luminosity function of GRBs could well be even wider (Loredo & Wasserman 1998b; Lamb 1999).

The general shape of the peak photon flux distributions $N_{\rm GRB}(P)$ can be understood as follows. The shape of $N_{\rm GRB}(P)$ above the rollover reflects the competition between the increasing number of GRBs expected at larger z (shown in Fig. 5) and their decreasing peak photon number flux $P(z)$ caused by their increasing distance, while the shape of $N_{\rm GRB}(P)$ below the rollover reflects the intrinsic luminosity function $f(L_P)$ of the bursts (Loredo & Wasserman 1998). The latter is particularly the case because cosmology causes the expected number of GRBs [$\propto N_*(z)$] to have an "edge" and, therefore, to be sharply peaked in z because of cosmology (Wasserman 1992). Thus, most of the GRBs below the rollover in the peak photon flux distribution

[3] The seven bursts with well-determined redshifts and published peak (isotropic) photon luminosities have a mean peak photon luminosity and sample variance $\log L_P = 58.1 \pm 0.7$.

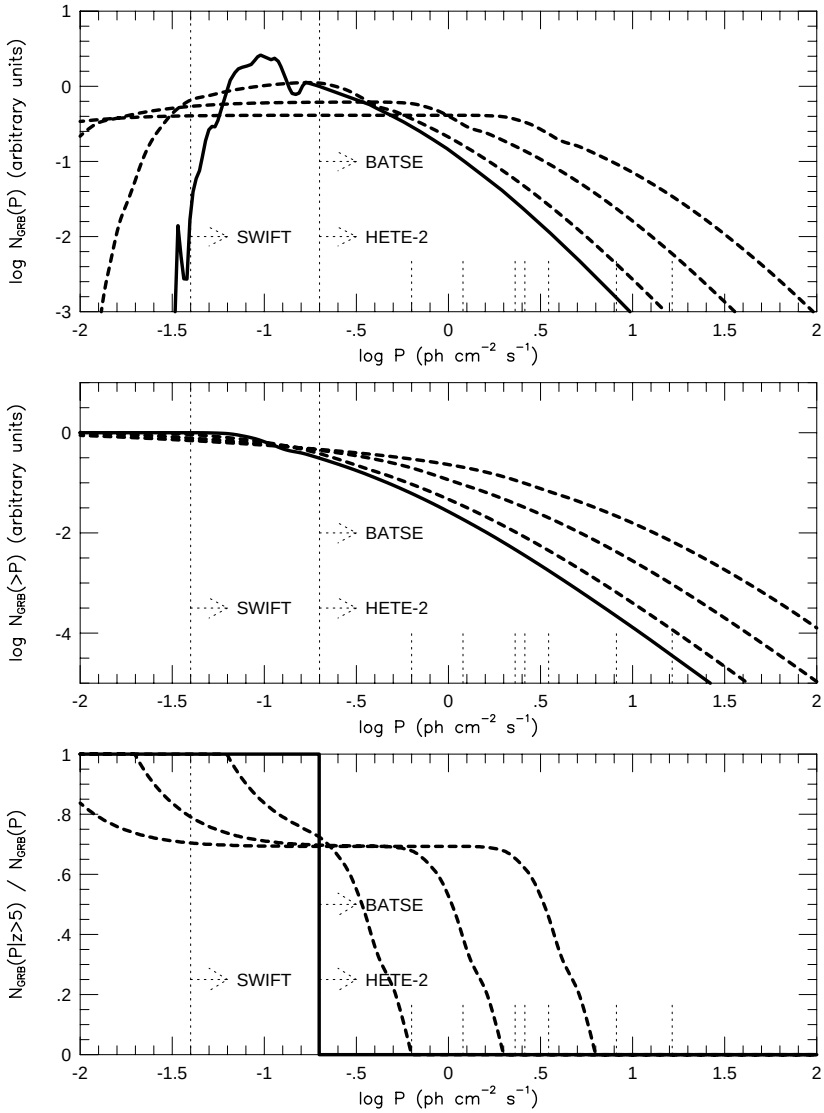

FIG. 6.—*Top panel:* Differential peak photon flux distribution of GRBs, assuming that (1) the GRB rate is proportional to the SFR; (2) the SFR is that shown in Fig. 5; and (3) the bursts are standard candles with a peak photon luminosity $L_P = 10^{58}$ photons cm^{-2} s^{-1} (*solid curve*) or have a logarithmically flat peak photon luminosity function that spans a factor of 10, 100, or 1000 (*dashed curves*). Approximate detection thresholds are plotted for BATSE and *HETE 2*, and for *Swift* (*dotted lines*). The dotted hashes mark the peak photon fluxes of the bursts from Table 1. *Middle panel:* Cumulative peak photon flux distribution of GRBs for the same luminosity functions. *Lower panel:* Fraction of GRBs with peak photon flux P that have redshifts of $z \gtrsim 5$ for the same luminosity functions.

$N_{GRB}(P)$ lie at the same distance ($z \approx 2$) but have a range of intrinsic peak flux luminosities L_P, reflecting the intrinsic luminosity function $f(L_P)$. This is particularly clear in Figure 6, where $N_{GRB}(P)$ is flat, and the plateau extends over an increasingly broad range of peak photon fluxes for increasingly broad intrinsic luminosity functions $f(L_P)$. It is also evident in Figures 7 and 8, where $N_{GRB}(P)$ below the rollover has slopes of ≈ -1 and ≈ -2.

Thus, information can be extracted from $N_{GRB}(P)$ about both the GRB rate as a function of redshift *and* the intrinsic luminosity function $f(L_P)$ of the bursts. Figures 6, 7, and 8 show that the limiting sensitivities of BATSE and *HETE 2*, and of *Swift*, all lie well below the observed rollover at $P \approx 6$ photons cm^{-2} s^{-1}. Therefore, BATSE has detected, and *HETE 2* will detect, many GRBs out to $z \approx 10$, if this picture is correct. *Swift* will detect many GRBs out to $z \approx 14$ and will also detect for the first time many intrinsically fainter GRBs.

The middle panels of Figures 6, 7, and 8 show the predicted cumulative peak photon flux distribution $N_{GRB}(>P)$ for the same set of luminosity functions. For the SFR we have assumed, we find that, if GRBs are assumed to be "standard candles," the predicted peak photon flux distribution falls steeply throughout the BATSE and *HETE 2* regime and therefore fails to match the observed distribution, in agreement with earlier work. In fact, we find that a photon luminosity function spanning at least a factor of 100 is required in order to obtain semiquantitative agreement with the principle features of the observed distribution; i.e., a rollover at a peak photon flux of $P \approx 6$ photons cm^{-2} s^{-1} and a slope above this of about $-3/2$. This implies that there are large numbers of GRBs with peak photon number fluxes below the detection threshold of BATSE and *HETE 2*, and even of *Swift*.

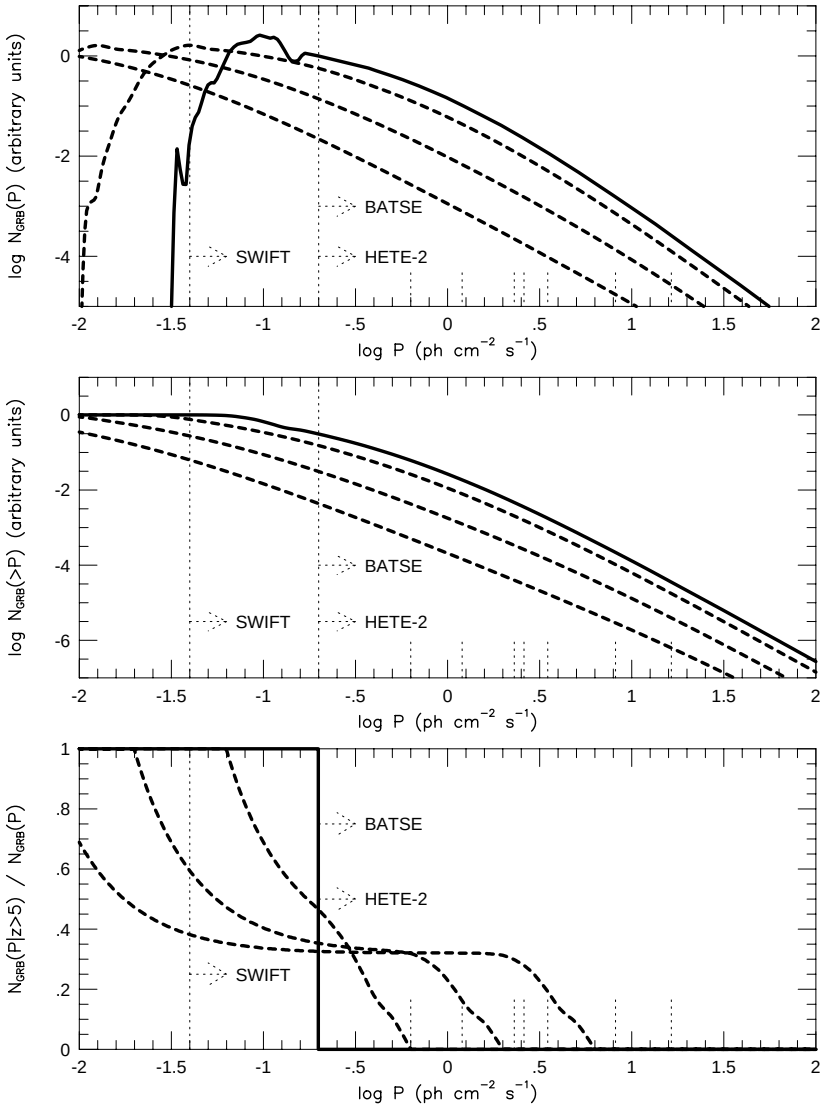

FIG. 7.—Same as Fig. 6, except that the dashed curves correspond to a power-law GRB luminosity function with slope $\beta = -1$

The lower panels of Figures 6, 7, and 8 show the predicted fraction of bursts with peak photon number flux P that have redshifts of $z > 5$, for the same set of luminosity functions. From these figures, we see that near the detection threshold of *Swift*, a significant number of bursts will have redshifts of $z > 5$. Depending on the slope and the width of the luminosity function, more than half of such bursts may have redshifts of $z > 5$.

4. GRBs AS A MEANS OF FINDING SUPERNOVAE AT VERY HIGH REDSHIFTS

GRBs can be used as beacons, revealing the locations of SNe at high redshifts ($z > 1$). To illustrate this, we take the best-fit V-band light curve of the early afterglow of GRB 970228 from Reichart (1999) and add to it the V-band (or peak spectral flux) light curve of SN 1998bw (Galama et al. 1998; McKenzie & Schaefer 1999), using the light curve of SN 1998bw as a template, as we did in Reichart (1999). The light curves we use are corrected for Galactic extinction, as explained in Reichart (1999). We then transform the two components to redshifts of $z = 1.2$, 3.0, 7.7, and 20, as described in § 2. Figure 9 shows the resulting light curves.

Figure 9 shows that, if a SN 1998bw-like event occurred at a redshift of $z \approx 3$, then it would peak in the K band about 70 days after the event, and the peak magnitude would be $K \approx 24.4$. Consequently, the detection of high redshift SNe—localized on the sky and in redshift by earlier GRB afterglow observations—is within the limits of existing ground-based instruments, and well within the limits of *HST*/NICMOS observations, out to a redshift of at least $z \approx 3$. At higher redshifts, SNe could be detected with NIR observations at frequencies above the peak frequency of the SN in the observer's frame; but because this portion of the SN spectrum is very red, the flux at NIR frequencies in the observer's frame decreases rapidly with increasing redshifts. Consequently, SNe at redshifts higher than $z \sim 4$ or 5 probably cannot be detected in the NIR using existing instruments. At still higher redshifts, one must appeal to L- and M-band observations, but existing instruments do not yet have the necessary sensitivity.

In Table 2, we expand upon Figure 9 by listing the band and the number of days after the GRB that observations would have the best chance of detecting a SN 1998bw-like event at peak flux density for a variety of GRB redshifts. We also list at

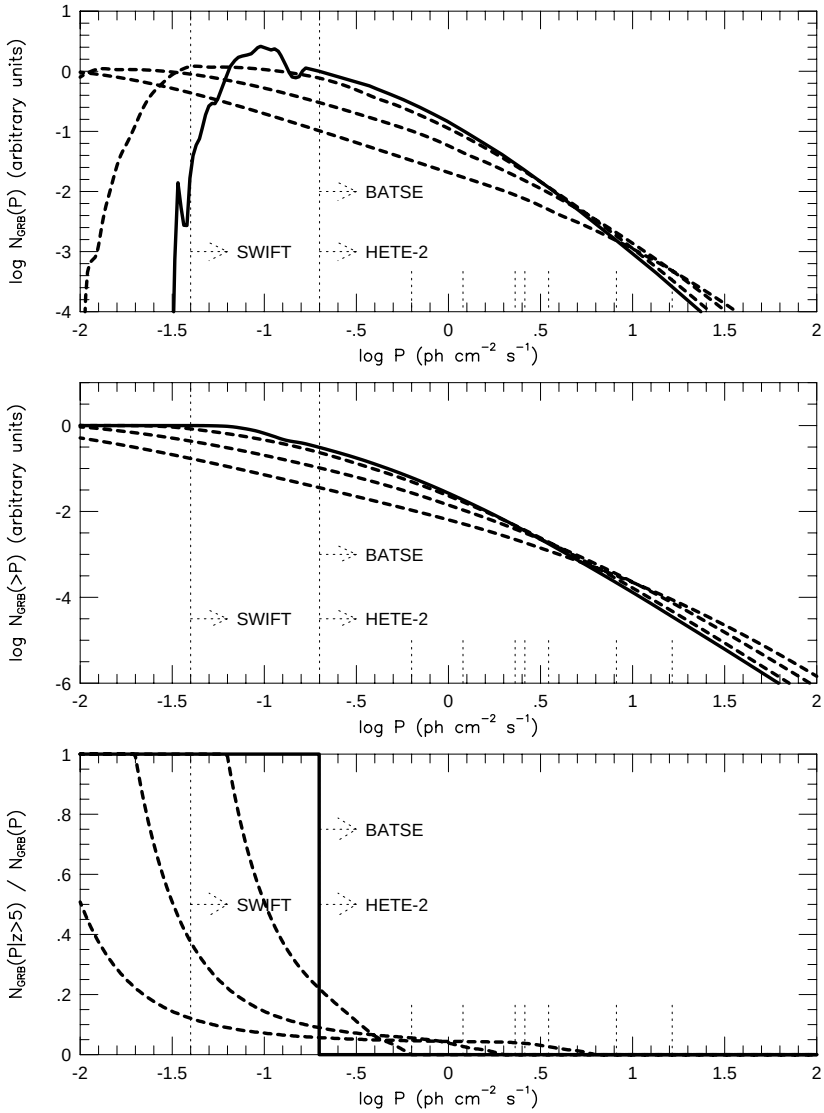

FIG. 8.—Same as Fig. 6, except that the dashed curves correspond to a power-law GRB luminosity function with slope $\beta = -2$

what magnitudes SN 1998bw would have been detected in these bands at these times if transformed to these redshifts. Of course, the chances of detecting a SN component depend on (1) how bright the afterglow is in the band of observation at the time of observation, (2) how bright the host galaxy, if detected, is in the band of observation, and (3) how much Galactic extinction there is in the direction of the GRB in the band of observation.

Already, one burst, GRB 971214, has been found to have a redshift, $z = 3.418$ (Kulkarni et al. 1998), that lies at the high end of the redshift range for which current instruments can detect a SN 1998bw-like SN. In the case of this burst, K-band

TABLE 2

BANDS, TIMES, AND MAGNITUDES AT WHICH A SN 1998bw-LIKE EVENT WOULD PEAK AT VARIOUS REDSHIFTS

Redshift	Band	Time (days)	Magnitude	Flux Density (μJy)
0.0.....	V	17	...	...
0.2.....	R	20	20.1	28
0.5.....	I	25	22.0	3.9
1.2.....	J	39	23.7	0.54
2.0.....	H	52	24.1	0.22
3.0.....	K	70	24.4	0.11
5.3.....	L	110	24.5	0.045
7.7.....	M	151	24.4	0.026

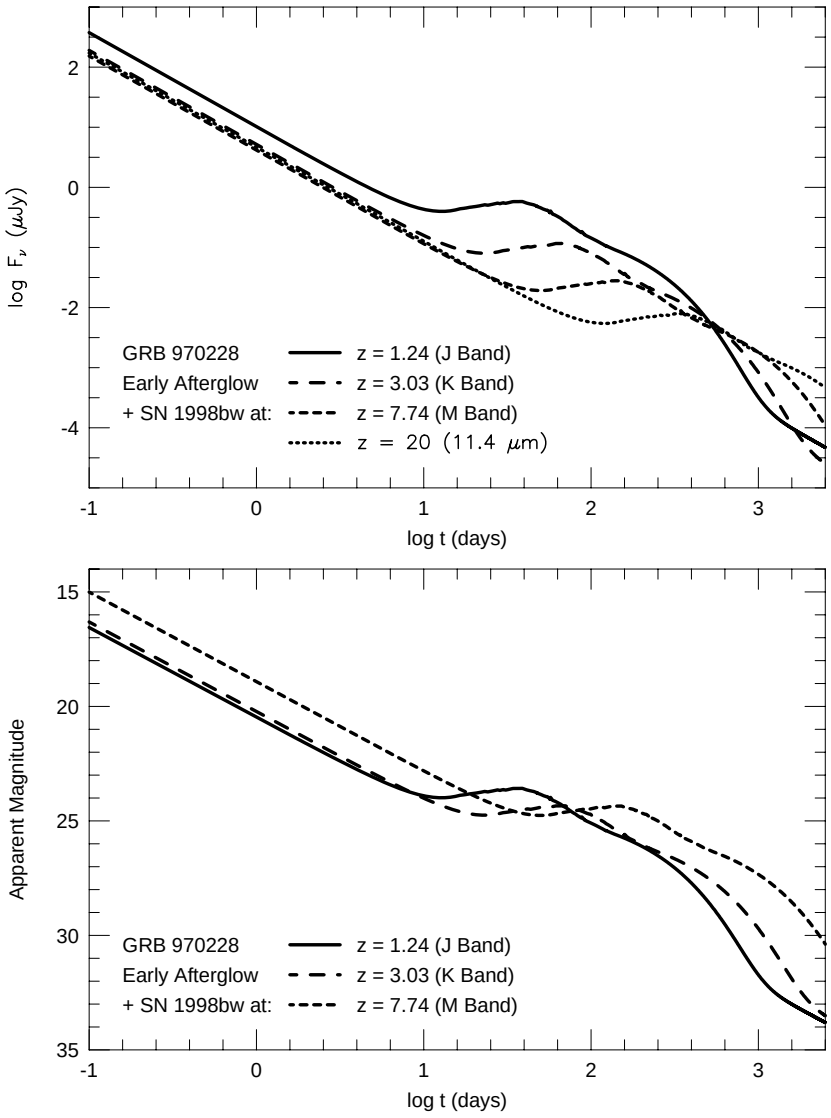

FIG. 9.—V-band, or peak flux density, light curve of SN 1998bw plus the corresponding best-fit light curve of the early afterglow of GRB 970228 from Reichart (1999), transformed to various redshifts and corrected for Galactic extinction along the SN 1998bw and GRB 970228 lines of sight (see § 4 for more details).

observations were taken 54 and 58 days after the burst (Ramaprakash et al. 1998), but these observations did not go deep enough to detect a SN component similar to SN 1998bw, were one present in the light curve.

As a further example, we consider the case of GRB 990510, a recent burst the afterglow of which faded as $t^{-2.4}$ (Stanek et al. 1999) or $t^{-2.2}$ (Harrison et al. 1999) at late times; the difference in these values can be traced to slight differences in these groups' respective parameterizations of the light curve of this afterglow (Harrison et al. 1999). As a consequence of this rapid fading, a SN 1998bw-like component to the light curve, if present, would dominate the afterglow after about a month at red and NIR wavelengths. Again using SN 1998bw as a template, we transform this template to the redshift of the burst, $z = 1.619$ (Vreeswijk et al. 1999) and correct this template for the difference in Galactic extinction ($A_V = 0.233$ mag versus $A_V = 0.673$ mag) along the SN 1998bw and GRB 990510 lines of sight using the dust maps of Schlegel, Finkbeiner, & Davis (1998)[4] and the Galactic extinction curve of Cardelli, Clayton, & Mathis (1989) for $R_V = 3.1$. We plot the resulting observer-frame I-, J-, H-, and K-band predictions for a SN 1998bw-like component of the afterglow of GRB 990510 at 49, 101, and 144 days after the burst in Figure 10.

If there is a SN component in the afterglow, it could easily have been detected with the NICMOS instrument on *HST*, had it not run out of cryogen half a year earlier. In the absence of NICMOS, Fruchter et al. (1999b) performed *HST*/STIS observations of the afterglow on 8.1 and 17.9 June 1999. They detected the afterglow at $V = 27.0 \pm 0.2$ mag and $V = 27.8 \pm 0.3$ mag on these two dates, which is consistent with the extrapolated light curve of the afterglow and, therefore, is not consistent with an additional SN 1998bw-like component in the afterglow (Fruchter et al. 1999b). However, caution is in order, since this conclusion is subject to a number of uncertainties. These include assumptions about (1) the spectral form of the afterglow at the times of the observations, since the observations spanned a wavelength range of 300–900 nm; (2) how to

[4] Software and data are available at http://astron.berkeley.edu/davis/dust/index.html.

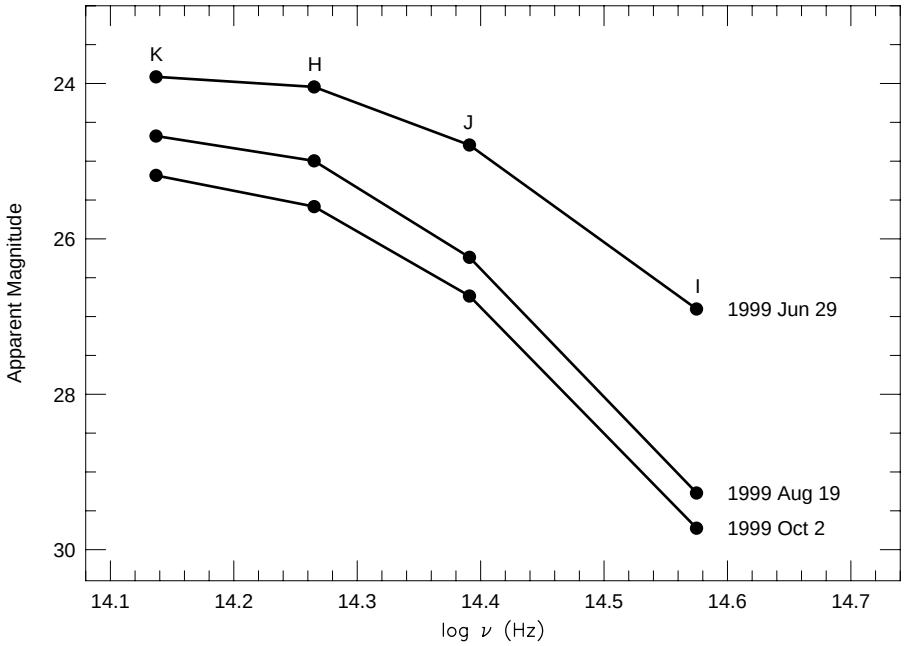

FIG. 10.—Spectral flux distributions of SN 1998bw, as observed 49, 101, and 144 days after the event, after transforming it to the redshift, $z = 1.619$ (Vreeswijk et al. 1999), of GRB 990510 and correcting it for differences in Galactic extinction along the SN 1998bw and GRB 990510 lines of sight.

extrapolate the light curve of the early afterglow of GRB 990510 to the times of the observations; (3) the luminosity of the supernova component relative to the luminosity of SN 1998bw, since Type Ib–Ic supernovae are known not to be standard candles; (4) the brightness of SN 1998bw at ultraviolet wavelengths; (5) the ignorability of any difference in host galaxy extinction along the SN 1998bw and GRB 990510 lines of sight; and (6) the underlying cosmological model.

5. MEASURING THE REDSHIFTS OF VERY HIGH REDSHIFT GRBs

Of the eight GRBs with secure redshifts, four have redshifts between $0.4 \lesssim z \lesssim 1$, two have redshifts between $1 \lesssim z \lesssim 2$, and one (GRB 971214) has a redshift of $z = 3.42$ (see Table 1). These redshifts have been found in two ways: (1) by taking a spectrum of the afterglow at early times, when the afterglow was still sufficiently bright (GRBs 970508, 980703, 990123, and 990510), and (2) by taking a spectrum of the host galaxy, if detected, at sufficiently late times, once the afterglow had faded (GRBs 970228, 970508, 971214, 980613, and 980703).

Both methods have uncertainties. In the former case, one technically measures only a lower limit for the redshift of the burst, corresponding to the redshift of the first absorber along the line of sight from the burst. However, as most, and possibly all, bursts with optical afterglows are associated with host galaxies, this first absorber is likely to be the host galaxy itself. Consequently, GRB redshifts measured in this way are fairly secure.

In the latter case, one must establish that the positional coincidence between the afterglow and the potential host galaxy is not accidental. For ground-based observations, $\approx 10\%$ of the sky is covered by galaxies brighter than $R \approx 25.5$, a typical magnitude for GRB host galaxies (see, e.g., Hogg & Fruchter 1999) because of seeing (Lamb 1999). Consequently, identification of the host galaxy is best established using *HST* images. In the cases of GRB 970508 (Metzger et al. 1997a, 1997b), GRB 980703 (Djorgovski et al. 1998), and GRB 990712 (Galama et al. 1999a), both absorption and emission lines were measured. (It is notable that the redshifts for the two GRBs at $z = 1.6$ were found by taking a spectrum of the GRB afterglow at early times. Currently, redshifts of host galaxies in the range $1 \lesssim z \lesssim 2.5$ are difficult to measure because the Hα and [O II] emission lines both lie outside the optical band for this range of redshifts.)

At VHRs, e.g., $z \gtrsim 5$, both methods will be challenging. Consider first the detection of absorption lines in afterglow spectra. In Figure 11, we plot the observed wavelengths of prominent absorption lines as a function of redshift. At VHRs, the prominent Balmer lines are redshifted out of the NIR and therefore out of the wavelength range of instruments such as NIRSPEC (0.9–5.1 μm; McLean et al. 1998). Prominent metal lines such as Mg II and Fe II are not redshifted out of the NIR. However, both observations (see, e.g., York 1999) and theoretical calculations (see, e.g., Ostriker & Gnedin 1996; Gnedin & Ostriker 1997; Valageas et al. 1999; Valageas & Silk 1999) suggest that the metallicity of the universe decreases with increasing redshift, especially beyond $z \gtrsim 3$. Therefore, the equivalent widths of the prominent metal lines are expected to decrease with increasing redshift, making them challenging to detect at very high redshifts.

However, prominent metal lines associated with the host galaxy may still be present if many GRBs are caused by the collapse of massive stars and the bursts occur near or in star-forming regions, since substantial production of metals would be expected in the disk—and certainly in the star-forming regions—of the host galaxy. This is illustrated by Figure 14 of Valageas & Silk (1999), which we have reprinted as Figure 12 in the present paper.

The second method, which requires detecting the potential host galaxy, confirming its identification as the host galaxy through positional coincidence with the GRB afterglow, and detecting Lyα, [O II], or other emission lines from the host galaxy, will also be challenging. This will be the case because (1) galaxies more massive than $\sim 10^9 M_\odot$ are not expected to

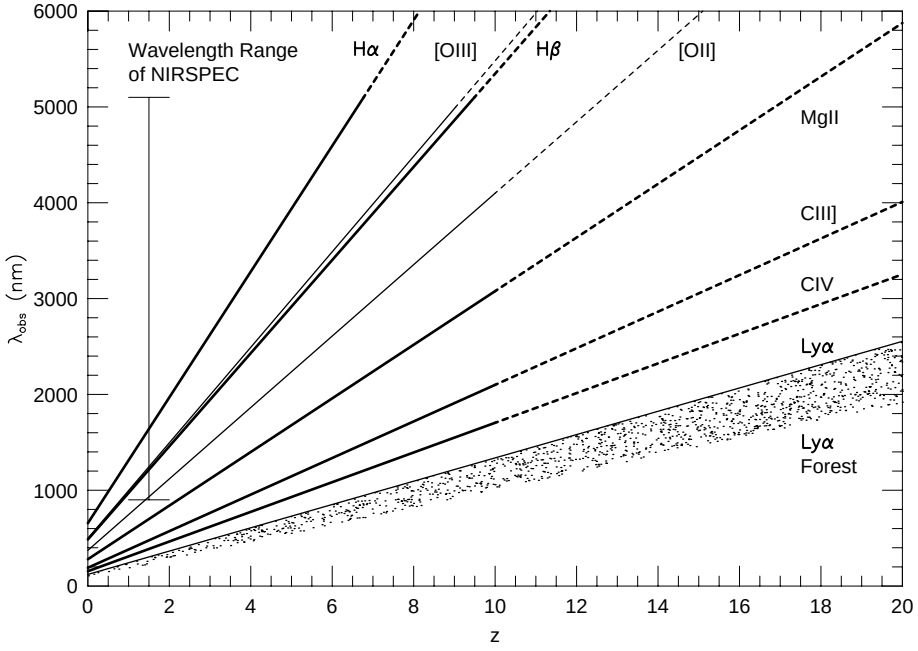

FIG. 11.—Observed wavelengths of prominent absorption lines and the Lyα forest as a function of redshift. At VHRs, the prominent Balmer lines will be difficult to detect because they will be shifted out of the NIR, and the prominent metal lines may be difficult to detect because of the low metallicity of the universe at these early times (see Fig. 12).

have formed by these times (see, e.g., Ostriker & Gnedin 1996; Gnedin & Ostriker 1997) and (2) because the surface brightness of these galaxies decreases as $(1 + z)^{-4}$. However, at redshifts $z \gtrsim 5$ (Fruchter 1999), and certainly at VHRs, the Lyα forest will be a very prominent feature of the spectral flux distribution of the GRB afterglow. This is evident in Figure 2, which shows the expected flux distribution of GRB afterglows at various redshifts. It is even more evident in Figure 13, which focuses in on NIR through optical frequencies.

As an illustration of this, consider a burst that occurs at a redshift slightly in excess of $z = 10$. If its afterglow is similar to that of GRB 970228, which had a relatively faint afterglow, its afterglow would be detectable at $K \approx 16.2$ mag one hour after the burst and at $K \approx 21.6$ mag one day after the burst. However, the afterglow would not be detectable in the J band to any

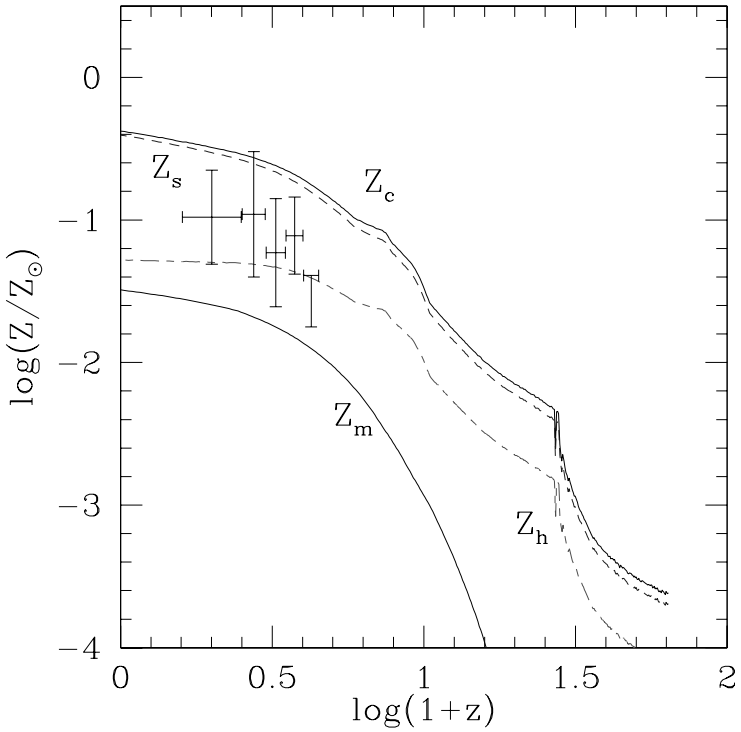

FIG. 12.—Fig. 14 of Valageas & Silk (1999): The redshift evolution of the metallicities Z_c (star-forming gas), Z_s (stars), Z_h (galactic halos), and Z_m (matter average). The data points are from Pettini et al. (1997b) for the zinc metallicity of damped Lyα systems.

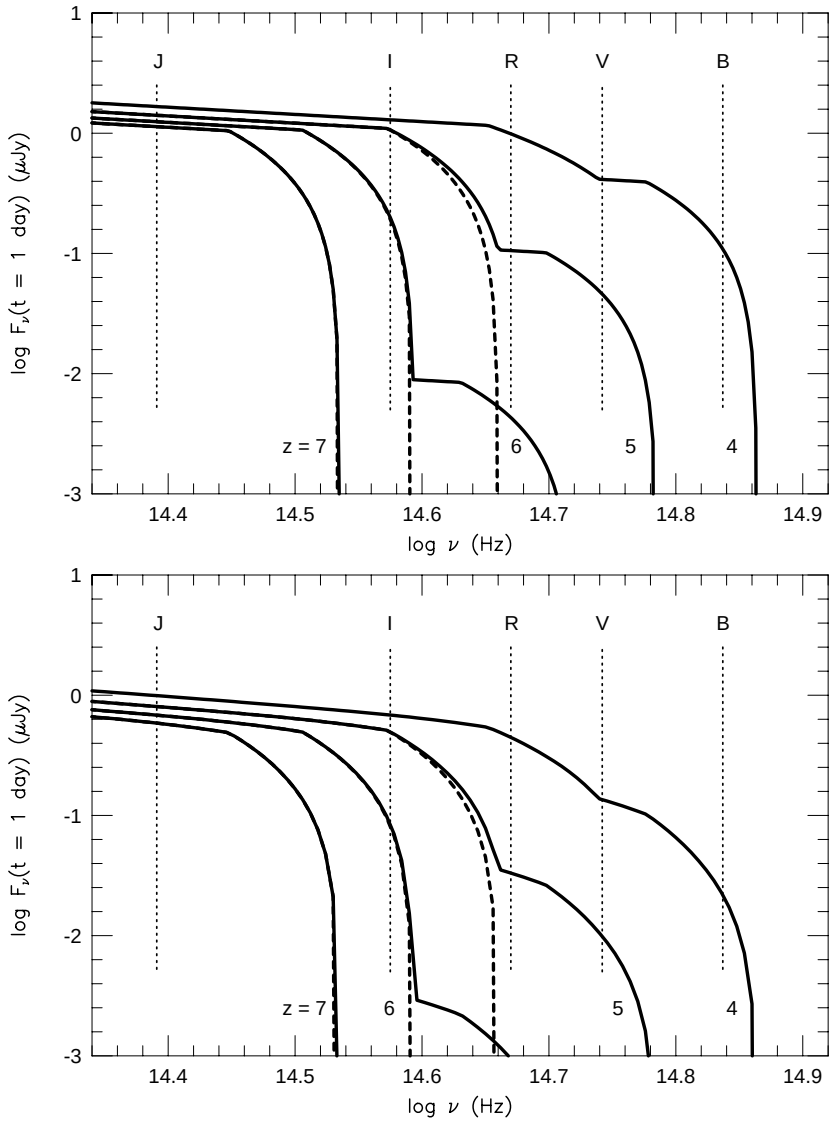

FIG. 13.—*Top panel:* The solid curves are the same as in Fig. 3; we assume that reionization occurred at a redshift in excess of $z = 7$. The dashed curves are the same as the solid curves, except that we instead assume that reionization occurred at a redshift of $4 < z < 5$. *Bottom panel:* The solid curves are the same as in the top panel, except extincted versions of the solid curves, where we have adopted $A_V = \frac{1}{3}$ mag at the redshift of the burst, and an extinction curve typical of the interstellar medium of our Galaxy (see § 7 for more details). The dashed curves are the same as the solid curves, except that we instead assume that reionization occurred at a redshift of $4 < z < 5$.

attainable limiting magnitude. Consequently, not only could VHR GRBs be detected and identified relatively easily using existing ground-based instruments, but given the extreme nature of this effect, accurate redshifts could be determined from photometry alone.

One possible concern is that dust along the line of sight through the star-forming region or the disk of the host galaxy could produce extinction (see, e.g., Reichart 1998, 2000) that can mimic the signature of the Lyα forest in the spectral flux distribution of the afterglow (Lamb et al. 1999). However, at VHRs ($z \gtrsim 5$), this possibility is less likely because of (1) the lower abundance of dust in the universe at these early times and (2) the increasing flux deficit of the Lyα forest with redshift. We illustrate this latter effect in the lower panel of Figure 13, in which we replot the upper panel of Figure 13, except that the solid curves correspond to extincted versions of the solid curves. In the lower panel of Figure 13, we have taken $A_V = \frac{1}{3}$ mag at the redshift of the burst, an extinction magnitude that may be typical of the disks of host galaxies (see, e.g., Reichart 1998), and we have adopted an extinction curve that is typical of the interstellar medium of our Galaxy, using the extinction curve parameterization of Reichart (2000). Figure 13 shows that, at redshifts higher than $z \approx 5$, the signature of the Lyα forest clearly dominates the signature of the extinction curve.

6. TRACING THE METALLICITY OF THE UNIVERSE USING GRB AFTERGLOWS

Recent studies of QSO absorption lines associated with damped Lyα systems (Lu et al. 1996; Prochaska & Wolfe 1997; Pettini et al. 1997a, 1997b) provide strong evidence that the metallicity of the universe decreases with increasing redshift and decreases dramatically beyond $z \approx 3$. Recent observations (Cowie et al. 1995) have confirmed earlier evidence for a forest of C IV and Si IV doublets associated with the forest of Lyα lines (Meyer & York 1987). Observations of these systems extend

to $z = 4.5$, higher than the redshifts of the damped Lyα systems observed to date. The detection of a forest of C IV and Si IV doublets, when combined with models of the ionization field from QSO radiation (see, e.g., Meiksin & Madau 1993; Cowie et al. 1995), suggests the existence of a floor under the abundances of heavy elements at roughly $10^{-2}\,M_{\odot}$, extending to the highest redshifts observed so far (Songaila 1997).

These various abundance determinations indicate that heavy elements exist in QSO absorption-line systems as early as $z = 5$, although at low levels, with a marked increase in the metallicity of these systems evident at $z \approx 3$. This metallicity history is consistent with an early universal contamination of primordial gas by massive stars, followed by a delay in forming additional heavy elements until $z \approx 3$ (Timmes, Lauroesch, & Truran 1995), and finally a rise to 0.1 $M_{\odot}$ abundances at $z = 2$. The abundances of, e.g., Ca and Fe inferred from QSO absorption-line systems do not show a further increase at $z < 1$ to fully solar values (Meyer & York 1992). This may be due (1) to the fact that the disks of galaxies comparable to the Milky Way, in which solar abundances exist, provide such a small cross section for absorption against background quasars, compared with dwarf galaxies (York 1999); (2) to the depletion of some heavy elements by warm and cold clouds in low-z galaxies (Pettini et al. 1997a); and (3) possibly to the fact that solar metal abundances may be anomalously large by about a factor of 3 (R. Mushotsky, 1999, private communication). It may be that all three of these factors play a role.

However, as we have seen, theoretical calculations of star formation in the universe predict that the earliest generation of stars occurs at redshifts $z \approx 15$–20 and that the SFR increases thereafter, peaking at $z \approx 2$–10 (Ostriker & Gnedin 1996; Gnedin & Ostriker 1997; Valageas & Silk 1999). One therefore expects substantial metal production at $z > 3$. The discrepancy between this expectation and the abundances deduced from observations of QSO absorption-line systems may reflect differences between the metallicity of galactic disks and star-forming regions and the metallicities of the hydrogen clouds in the halos of galaxies and/or in the IGM that are responsible for QSO absorption lines.

This possibility is supported by Figure 12, taken from Valageas & Silk (1999), which shows the redshift evolution of the metallicities of (1) star-forming regions, (2) stars, (3) gas in galactic halos, and (4) the overall average metallicity of matter given by their model calculations. Also shown are the data points from Pettini et al. (1997b) for the metallicity of 34 damped Lyα systems, as inferred from zinc absorption lines. The curve corresponding to the overall average metallicity of matter represents an upper bound for the mean metallicity of the IGM (corresponding to very efficient mixing). If galaxies do not eject metals very extensively into the IGM, the metallicity of the IGM could be much smaller.

Figure 12 shows that the mean metallicity expected for star-forming regions is substantially more than that expected for clouds in the IGM and for Lyα clouds associated with galactic halos (Lyman limit or damped Lyα systems). Consequently, it is possible that the equivalent widths (EWs) of the absorption lines associated with the host galaxy of the GRB (if it occurs in a galaxy) will remain large at very high redshifts, even as the EWs of the absorption lines due either to gas clouds in the IGM or associated with the halos of galaxies weaken greatly beyond $z \approx 3$. The situation at still higher redshifts, where star formation may occur in globular cluster-sized entities but not in galaxies—which have not yet had time to form—is unclear.

It is clear from this discussion that studies of absorption-line systems in GRB afterglow spectra can contribute greatly to our understanding of the metallicity history of the universe and can allow a comparison between the metallicity history of hydrogen clouds along the line of sight to the burst *and* the metallicity history of the star-forming regions and/or disks of the burst host galaxies (and the globular cluster-sized objects in which GRBs may occur at still higher redshifts).

Core-collapse SNe, such as the Type Ib–Ic SNe with which GRBs may be associated, produce different relative abundances of various metals than do Type Ia SNe, which are thought to be caused by the thermonuclear disruption of white dwarfs (see, e.g., Woosely & Weaver 1986). For example, the spectrum of SN 1998bw, a peculiar Type Ic SN, exhibited absorption lines reflecting the production of substantial amounts of O and Cr, as well as Mg II, Fe, Ca, Si, and some S (Iwamoto et al. 1998; Mazzoli et al. 2000). This is typical of core-collapse SNe (i.e., Type Ib–Ic and Type II SNe). Thus the relative abundances of various heavy elements can also give clues about the origin of these elements; i.e., whether or not the metallicity is caused primarily by Type Ib–Ic and Type II SNe (core-collapse SNe) and when and at what rate Type Ia SNe begin to contribute to the increase in metallicity.

Finally, studies of the absorption lines in GRB afterglow spectra can help to determine whether the ratio [Fe/H] is a good chronometer at high redshift, as has usually been assumed, or may not be, as recent studies have suggested (J. Truran, 1999, private communication). Such studies can also help to determine the extent and importance of mixing between the metals and the hydrogen gas in galaxies and in the IGM.

7. GRBs AND THEIR AFTERGLOWS AS PROBES OF LARGE-SCALE STRUCTURE

GRBs can be used to probe the large-scale structure of luminous matter in the universe (Lamb & Quashnock 1993; Quashnock 1996). The use of GRBs for this purpose has the advantage that they occur and are detectable out to VHRs, if GRBs are related to the collapse of massive stars. Thus observations of GRBs can be used to probe the properties of large-scale structure at much higher redshifts (and much earlier) than those that are currently probed by observations of galaxies and QSOs. GRBs also have the advantage that, while galaxy and QSO surveys on the largest angular scales face difficulties because of the absorption of light by dust and gas in the Galaxy, the Galaxy is completely transparent to gamma rays. Thus one can obtain a homogeneous sample of GRBs covering the entire sky, unlike existing and future galaxy and QSO surveys.

On the other hand, the use of GRBs to probe large-scale structure suffers from a very serious disadvantage, namely, small number statistics. *HETE 2* is expected to lead to the determination of the redshifts of a hundred or so bursts, while the *Swift* mission is likely to lead to the determination of the redshifts of $\sim$1000 bursts. These numbers are an order of magnitude smaller than the number of QSOs for which redshifts are currently known, which is itself far smaller than the number of QSO redshifts expected from the Sloan Digital Sky Survey. Thus the use of GRBs themselves as a tracer of large-scale structure in the universe may not be particularly powerful.

However, it should be possible to use the metal absorption lines and the Lyα forest seen in the optical and infrared spectra of GRB afterglows to probe the clustering of matter on the largest scales, as has been done using these same lines in the optical spectra of QSOs (Quashnock, Vanden Berk, & York 1996; Quashnock & Vanden Berk 1998; Quashnock & Stein 1999). Deep images of fields around QSOs with absorbers in their spectra have revealed galaxies in the vicinities of absorbers and at the same redshifts (see, e.g., Steidel, Dickenson, & Persson 1994; Steidel et al. 1997). A similar association also has been inferred for a substantial fraction of the damped Lyα absorption lines (Lanzetta et al. 1995; Le Brun, Bergeron, & Boissé 1996). Consequently, it is thought that metal absorption lines are associated with galaxy halos and, possibly, galactic disks in some cases.

As discussed in §§ 2 and 3, we expect both GRBs and their afterglows to occur and to be detectable out to very high redshifts ($z > 5$), redshifts that are far larger than the redshifts expected for the most distant quasars. Consequently, the observation of absorption-line systems and damped Lyα systems in the optical and infrared spectra of GRB afterglows affords an opportunity to probe the properties of these systems and their clustering at VHRs.

At VHRs, one expects to be in the linear regime and that the mass spectrum of the Lyα forest systems, which are thought to lie in the IGM and possibly the damped Lyα systems, to follow the Harrison-Zeldovich spectrum of density fluctuation in the early universe. Observations of NIR and infrared absorption lines in the afterglow spectra of GRBs may allow one to test this expectation, provided that these lines are detectable. The decrease in metallicity with increasing redshift may make it difficult to detect absorption-line systems at redshifts $z \gtrsim 5$, but this may not be true for damped Lyα systems and the Lyα forest.

8. GRB AFTERGLOWS AS A PROBE OF THE EPOCH OF REIONIZATION

The epoch of reionization is one of the most important unknown quantities relevant to large-scale structure and cosmology. The lack of Gunn-Peterson absorption implies that this epoch lies at $z > 5$, while the lack of distortion of the microwave background by Compton scattering off of free electrons implies that it lies at $z < 50$. It is plausible to have reionization occur anywhere between these redshifts in most cosmological models. Observations of the afterglows of VHR GRBs can be used to constrain the epoch of reionization by the presence or absence of flux shortward of the Lyman limit in the rest frame of the GRBs (see Fig. 13).

The absence of Gunn-Peterson troughs (Gunn & Peterson 1965) in the spectra of high-redshift quasars (Schneider, Schmidt, & Gunn 1991) and galaxies (Franx et al. 1997) indicates that the IGM was reionized at a redshift in excess of $z \approx 5$. Whether reionization was caused by the first generation of stars or by quasars is not yet known. Assuming reionization was caused by the first generation of stars, Gnedin & Ostriker (1997) predict that reionization occurred at $z \approx 7$; assuming reionization was caused by quasars, Valageas & Silk (1999) predict that reionization occurred at $z \approx 6$. However, Haiman & Loeb (1998), assuming that reionization was caused by stars and/or quasars, predict that reionization occurred at a redshift in excess of $z \approx 11.5$.

Observations of VHR GRB afterglows may make it possible to distinguish between these possibilities. If reionization occurred at a redshift of $z \lesssim 6$, as Valageas & Silk (1999) predict, then the redshift of reionization could be measured directly from VHR GRB afterglow photometry. We show this in Figure 13, in which we replot the spectral flux distributions shown in Figure 3, assuming that the intergalactic medium was not reionized until a redshift of $4 < z < 5$ (*dashed curves*). If reionization occurred at a redshift in excess of $z \approx 6$, as Gnedin & Ostriker (1997) and Haiman & Loeb (1998) predict, then observations of the afterglows of VHR GRBs could be used to probe the redshift evolution of the Lyα forest out to this redshift using existing ground-based instruments. However, to reach $z \approx 6$, observations would have to commence within a few hours of, instead of ≈ 1 day after, a burst. The *HETE 2* and *Swift* missions, which will provide burst positions accurate to a few arcseconds in near-real time, should make such observations possible. Future advances in instrumentation should allow redshifts in excess of $z \approx 6$ to be probed.

9. CONCLUSIONS

The work of Bloom et al. (1999) in the case of GRB 980326, and the subsequent work of Reichart (1999) and Galama et al. (1999b) in the case of GRB 970228, strongly suggest that at least some GRBs are related to the supernovae of massive stars. If many GRBs are related to the collapse of massive stars, we have shown that the bursts and their afterglows can be used as a powerful probe of many aspects of the very high redshift ($z \gtrsim 5$) universe.

We have established that both GRBs and their afterglows are detectable out to very high redshifts. *HETE 2* should detect GRBs out to $z \approx 30$, while the *Swift* mission would be capable of detecting GRBs out to $z \gtrsim 70$, although it is unlikely that bursts occur at such extremely high redshifts.

We have shown that, on the basis of theoretical calculations of star formation in the universe, one expects GRBs to occur out to at least $z \approx 10$ and possibly to $z \approx 15$–20, redshifts that are far larger than those expected for the most distant quasars. This implies that there are large numbers of GRBs with peak photon number fluxes below the detection thresholds of BATSE and *HETE 2*, and even below the detection threshold of *Swift*. It also implies that *HETE 2* will detect many GRBs out to $z \approx 8$. Similarly, the *Swift* mission would detect many GRBs out to $z \approx 14$ and would detect for the first time many intrinsically fainter GRBs. The mere detection of VHR GRBs would give us our first information about the earliest generations of stars. We have shown how GRBs and their afterglows can be used as beacons to locate core-collapse supernovae at redshifts $z \gg 1$ and to study the properties of these supernovae.

We have described the expected properties of the absorption-line systems and the Lyα forest in the spectra of GRB afterglows. We have described and compared various strategies for determining the redshifts of very high redshift GRBs. We have shown how the absorption-line systems and the Lyα forest visible in the spectra of GRB afterglows can be used to trace the evolution of metallicity in the universe and to probe the large-scale structure of the universe at very high redshifts. Finally,

we have shown how measurement of the Lyα break in the spectra of GRB afterglows can be used to constrain, or possibly measure, the epoch at which reionization of the universe occurred using the Gunn-Peterson test.

This research was supported in part by NASA grant NAG5-2868 and NASA contract NASW-4690. We thank Carlo Graziani for discussions about the proper way to calculate GRB peak photon flux and peak photon energy distributions. We thank Don York for discussions about QSO metal absorption-line systems and the metallicity history of the universe and Jean Quashnock for discussions about using QSO absorption-line systems to probe the large-scale structure of the universe. We thank Jim Truran for discussions about whether [Fe/H] is a good chronometer at early times in the evolution of the Galaxy and at high redshift. Finally, we thank Dave Cole for providing information about the limiting magnitudes that are detectable using current NIR instruments.

REFERENCES

Bloom, J. S., et al. 1998, ApJ, 507, L25
———. 1999, Nature, 401, 453
Cardelli, J. A., Clayton, G. C., & Mathis, J. S. 1989, ApJ, 345, 245
Castander, F. J., & Lamb, D. Q. 1998, in Gamma-Ray Bursts, ed. C. A. Meegan, R. D. Preece, & T. M. Koshut (New York: AIP), 520
———. 1999, ApJ, 523, 593
Connolly, A. J., et al. 1997, ApJ, 486, L11
Costa, E., et al. 1997, IAU Circ. 6572
Cowie, G. L., et al. 1995, AJ, 109, 1522
Djorgovski, S. G., et al. 1998, ApJ, 508, L17
———. 1999a, GCN Circ. 189 (http://gcn.nasa.gov/gcn/gcn3/189.gcn3)
———. 1999b, GCN Circ. 289 (http://gcn.nasa.gov/gcn/gcn3/289.gcn3)
Franx, M., et al. 1997, ApJ, 486, L75
Frail, D. A., & Kulkarni, S. R. 1997, IAU Circ. 6662
Fruchter, A. S. 1999, ApJ, 516, 683
Fruchter, A. S., et al. 1999a, ApJ, 516, 683
———. 1999b, GCN Circ. 386 (http://gcn.nasa.gov/gcn/gcn3/386.gcn3)
Galama, T. J., et al. 1997, IAU Circ. 6584
———. 1998, Nature, 395, 670
———. 1999a, GCN Circ. 388 (http://gcn.nasa.gov/gcn/gcn3/388.gcn3)
———. 1999b, ApJ, 536, 185
Gallego, J. 1995, ApJ, 455, L1
Gehrels, N. 1999, BAAS, 31, 993
Gnedin, N. Y., & Ostriker, J. P. 1997, ApJ, 486, 581
Gorosabel, J., et al. 1998, A&A, 335, L5
Graziani, C., Lamb, D. Q., & Marion, G. H. 1999, ApJ, submitted, preprint (astro-ph/9810374)
Gunn, J. E., & Peterson, B. A. 1965, ApJ, 142, 1633
Haiman, Z., & Loeb, A. 1998, ApJ, 503, 505
Halpern, J. P., et al. 1999, ApJ, 517, L105
Harrison, F. A., et al. 1999, ApJ, 523, L121
Hogg, D. W., & Fruchter, A. S. 1999, ApJ, 520, 54
Iwamoto, K., et al. 1998, Nature, 395, 672
Kouveliotou, C., et al. 1993, ApJ, 413, L101
Kulkarni, S. R., et al. 1998, Nature, 395, 663
———. 1999, Nature, 398, 389
Lamb, D. Q. 1999, A&AS, 138, 607
Lamb, D. Q., Castander, F. J., & Reichart, D. E. 1999, A&AS, 138, 479
Lamb, D. Q., Graziani, C., & Smith, I. A. 1993, ApJ, 413, L11
Lamb, D. Q., & Quashnock, J. M. 1993, in Gamma-Ray Bursts, ed. M. Friedlander, N. Gehrels, & D. Macomb (New York: AIP), 1025
Lanzetta, K. M., et al. 1995, ApJ, 440, 435
Le Brun, V., Bergeron, J., & Boissé, P. 1996, A&A, 306, 691
Lilly, S. J., et al. 1996, ApJ, 460, L1
Loredo, T. J., & Wasserman, I. M. 1998, ApJ, 502, 108
Lu, L., et al. 1996, ApJS, 107, 475
MacFadyen, A. I., & Woosley, S. E. 1999, ApJ, 524, 262
MacFadyen, A. I., Woosley, S. E., & Heger A. 1999, ApJ, submitted, preprint (astro-ph/9910034)
Madau, P., Pozzetti, L., & Dickinson, M. 1998, ApJ, 498, 106
Mallozzi, R. S., Pendleton, G. N., & Paciesas, W. S. 1996, ApJ, 471, 636
Mazzoli, P. et al. 2000, ApJ, submitted
McKenzie, E. H., & Schaefer, B. E. 1999, PASP, 111, 964
McLean, I. S., et al. 1998, Proc. SPIE, 3354, 566
Meiksin, A., & Madau, P. 1993, ApJ, 412, 34
Mészáros, P., & Rees, M. J. 1992, ApJ, 397, 570
Metzger, M. R., et al. 1997a, IAU Circ. 6631
———. 1997b, Nature, 387, 878
Meyer, D. M., & York, D. G. 1987, ApJ, 319, L45
———. 1992, ApJ, 399, L121
Narayan, R., Paczyński, B., & Piran, T. 1992, ApJ, 395, L83
Ostriker, J. P., & Gnedin, N. Y. 1996, ApJ, 472, L63
Paciesas, W. S., et al. 1999, ApJS, 122, 465
Paczyński, B. 1986, ApJ, 308, L43
———. 1998, ApJ, 494, L45
Pei, Y. C., Fall, S. M., & Hauser, M. G. 1999, ApJ, 522, 604
Pettini, M., et al. 1997a, ApJ, 478, 536
———. 1997b, ApJ, 486, 665
Prochaska, J. X., & Wolfe, A. M. 1997, ApJ, 474, 140
Quashnock, J. M. 1996, ApJ, 461, L69
Quashnock, J. M., & Stein, M. L. 1999, ApJ, 515, 506
Quashnock, J. M., & Vanden Berk, D. E. 1998, ApJ, 500, 28
Quashnock, J. M., Vanden Berk, D. E., & York, D. G. 1996, ApJ, 472, L69
Ramaprakash, A. N., et al. 1998, Nature, 393, 43
Reichart, D. E. 1998, ApJ, 495, L99
———. 1999, ApJ, 521, L111
———. 2000, ApJ, submitted, preprint (astro-ph/9912368)
Ricker, G. 1998, BAAS, 30, Abstract 33.14
Rowan-Robinson, M. 1999, Astroph. & Space Sci., in press (astroph/9906308)
Sahu, K. C., et al. 1997, Nature, 387, 476
Schlegel, D. J., Finkbeiner, D. P., & Davis, M. 1998, ApJ, 500, 525
Schneider, D. P., Schmidt, M., & Gunn, J. E. 1991, AJ, 102, 837
Songaila, A. 1997, ApJ, 490, L1
Stanek, K. Z., et al. 1999, ApJ, 522, L39
Steidel, C. C., et al. 1997, ApJ, 480, 568
Steidel, C. C., Dickenson, M., & Persson, S. E. 1994, ApJ, 437, L75
Timmes, F. X., Lauroesch, J. T., & Truran, J. W. 1995, ApJ, 451, 468
Totani, T. 1997, ApJ, 486, L71
———. 1999, ApJ, 511, 41
Valageas, P., Schaeffer, R., & Silk, J. 1999, A&A, 345, 691
Valageas, P., & Silk, J. 1999, A&A, 347, 1
Vreeswijk, P. M., et al. 1999, GCN Circ. 324 (http://gcn.nasa.gov/gcn/gcn3/324.gcn3)
Wasserman, I. 1992, ApJ, 394, 565
Wheeler, J. C., et al. 2000, ApJ, 537, in press
Wijers, R. A. M. J., et al. 1998, MNRAS, 294, L13
Wijers, R. A. M. J., Rees, M. J., & Mészáros, P. 1997, MNRAS, 288, L51
Woosley, S. E. 1993, ApJ, 405, 273
———. 1996, in Gamma-Ray Bursts, ed. C. Kouveliotouo, M. Briggs, & G. Fishman (New York: AIP), 709
Woosley, S. E., & Weaver, T. A. 1986, ARA&A, 24, 205
York, D. G. 1999, in ASP Conf. Proc. 166, Stromlo Workshop on High-Velocity Clouds, ed. B. K. Gibson & M. E. Putman (San Francisco: ASP), 188
Zuo, L., & Lu, L. 1993, ApJ, 418, 601